Implementation of a GNU Radio and Python FMCW Radar Toolkit

Themba W. Mathumo*†, Theo G. Swart* and Richard W. Focke†
*Depart. of Electrical and Electronic Engineering Science, University of Johannesburg, South Africa
†Defence, Peace, Safety and Security, Council for Scientific and Industrial Research, South Africa
tmathumo@csir.co.za, tgswart@uj.ac.za, rfocke@csir.co.za

Abstract*—The use of GNU Radio in order to explore FMCW radar is growing rapidly, where it is used for radar signal processing. In this paper we implement FMCW surveillance radar for drone detection on SDR using GNU Radio and the USRP B210. The requirement was to design and implement an FMCW surveillance radar to detect a drone with a radar cross-section of 0.1 m^2 and a maximum range of 150 m for the purpose of point detection. The signal processing takes the beat frequency which has pulse compression gain and performs coherent integration. It windows and displays the results on a range Doppler map using two-dimensional fast Fourier transform. The pulse repetition frequency of the waveform is selected as 2200 Hz with a chirp bandwidth of 28 MHz, allowing for resolving a maximum velocity of 30 m/s unambiguously, which is the typical maximum speed of a small drone. Experiments were conducted using a human being and a car target as a drone was not available. The B210 induced a phase drift in the results which causes a Doppler shift. The phase drift was resolved by creating a phase equalization matrix, which was used to correct the phase drift in real-time. Verification of the designed radar system yielded a 63% probability of detection and probability of false alarm of 1.7×10^{-6}.

***Index Terms*—Doppler radar, frequency modulation, radar signal processing, software defined radar**

I. Introduction

There is a growing demand for cheap portable radar systems which are configurable and can be used for different applications. Typical examples are for medical imaging [1] and synthetic aperture radar (SAR) [2].

Software defined radio (SDR) is a radio transceiver in which most of the key parameters of radio operations, that are typically implemented in hardware, are implemented in software. SDR has allowed radar to be explored in software [3]. Radar is primarily used to measure range and radial velocity using transmission and reception of radio frequency (RF) and signal processing. GNU Radio is one of the platforms that is used for designing software defined radar together with the Universal Software Radio Peripheral (USRP) as front end.

Ralston and Hargrave [3] introduce ground penetrating radar (GPR) and the concept of using SDR for radar ranging. The requirements for GPR radar are usually high bandwidth, timing accuracy and high transmit power. The prototype was built using GNU Radio and USRP2 since these are open source and generic.

Sundaresan *et al.* [4] discuss SDR radar as a potential technology to be used for target detection and tracking. Prabaswara *et al.* [5] discuss the use of SDR radar for weather surveillance purposes. Both studies have a similar implementation: USRP N210 and GNU Radio are used in their conceptual designs using FMCW waveform.

Research and development on Reconfigurable Hardware Interface for Computation and Radio (RHINO) is being done at the University of Cape Town [6]. RHINO is an open source development consisting of hardware and software which is also designed for radar application. Such hardware opens the opportunity for the practical realization of radar.

The application area of drone detection is of interest as drones are gaining popularity in transportation and are also increasingly being used for criminal purposes, such as spying and transportation of drugs into prison [7]. Thus, it is of interest to determine whether SDR is capable of being used for radar surveillance applications, as it could lead to radar systems deployable against the increasingly prevalent drones.

II. FMCW Waveforms

Frequency-modulated continuous-wave (FMCW) radar has been the center of interest when designing radar in GNU Radio because of its low power requirements and low cost [5]. An FMCW waveform, also known as a chirp, is modeled as [8]:

$$f(t) = f_T + \frac{f_{\text{dev}}}{T}t, \tag{1}$$

where $f(t)$ is the transmitted waveform of a center transmit frequency f_T plus the slope. The slope is the relationship between f_{dev} and T, where f_{dev} is the stop frequency of the chirp in hertz. Fig. 1 shows the reflected signal from a moving target, where the signal shifts up or down because of the Doppler effect. The problem is that the beat frequency consists of the Doppler and/or range component, and it is impossible to determine them using only one beat frequency.

A. Two-dimensional Signal Processing for FMCW Radar

Since it is not possible to determine both range and velocity using a single up/down chirp, and since the triangular chirp does not work for multiple targets, the double fast Fourier transform (FFT) technique for FMCW signal processing is used for multiple targets, as shown in Fig. 2.

The chirp sequence is multiple pulses within a coherent processing interval (CPI), and T_{CPI} is the dwell time at which a number of pulses are transmitted and received. The transmitted signal is mixed with the Doppler-shifted and time-delayed reflected signal. The M pulses are arranged in a

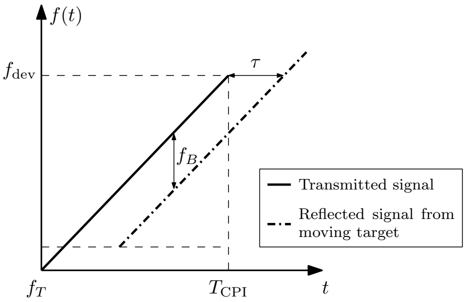

Fig. 1. Up chirp transmitted waveform with time-delayed reflected waveform from a stationary target [9].

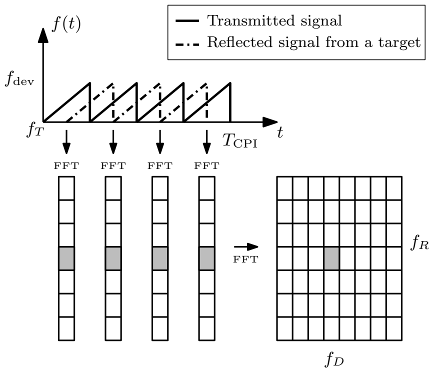

Fig. 2. Chirp processing by the method of pulse Doppler processing.

two-dimensional matrix in which range and Doppler FFT processing is performed in order to obtain a range Doppler matrix. Then the double FFT can be performed on the range Doppler matrix in order to obtain the range and radial velocity of targets.

III. System Design

The user requirement is to design and implement an FMCW ground-based surveillance radar. It should be able to detect small drones for the purpose of point defence, which is a low-range application, and have the following properties:

- A range coverage of up to 150 m—the maximum range allows time for detection and decision making after the target has been identified.
- Probability of detection of 80% is required for a 0.1 m^2 target, with probability of false alarm of 10^{-6}, meaning 1 false alarm per 1 million observations.
- The sampling rate that we could achieve using the B210 is 28 MHz, which results in the range resolution to be 5.35 m, and not 0.1 m as expected using the range resolution equation [10].
- A desired azimuth coverage of 45°. The advantage of using a directional antenna is that the antenna can achieve higher gain, the narrower the antenna the higher the gain. A drone is relatively small, thus the 45° azimuth coverage is enough for the radar to cover multiple drones in the direction that the radar is facing.

The performance of the low-cost USRP B210 transceiver is investigated for its performance for radar use in the C band. At the time of these investigations there was no previous radar work done using the B210.

A. Radar Waveform Design

The radar is designed based on user requirements which are then interpreted to be the design parameters using signal design rules [10]. The given user parameters are that the surveillance radar should be able to detect a drone as far as away as 150 m. The parameters are given in Table I. The design parameters were calculated using the above-mentioned signal design rules. The user parameters were adjusted depending on the constraints imposed by the B210 and the result of waveform design. Instead of having range resolution of 0.1 m, the achieved range resolution is 5.35 m because of the maximum bandwidth achieved by the B210; the velocity resolution that was expected by the user is 1 m/s but only 1.2 m/s was achieved based on the chosen pulse repetition frequency (PRF).

B. Radar Model

Table II gives the specifications of the USRP B210 and the antenna available that can be used for the experiments. Only the important parameters which are used to determine the radar performance are listed.

The radar characteristics are used to predict the radar performance by evaluating the SNR vs. range, as shown in Fig. 3. The SNR vs. range will be improved in order to meet the radar performance requirements.

The signal return of interest is buried under the noise floor since the SNR is negative. This means that during detection we will not be able to detect the targets.

The receiver operating characteristic (ROC) curve in Fig. 4 shows that in order to meet the user's performance requirement the SNR has to be 12 dB. Various techniques such as introducing amplifiers, the use of coherent integration and Doppler

TABLE I
The user parameters and the calculated design parameters

User Parameter	Value	Design Parameter	Value
Center frequency	5.5 GHz	PRF	2200
Range	Required: 150 m	Number of pulses	50
Range resolution	Required: 0.1 m, achievable: 5.35 m.	Range of samples	227
Velocity	30 m/s	Bandwidth	28 MHz
Velocity resolution	Required: 1 m/s, achievable: 1.2 m/s.	CPI=$\frac{\#\text{pulses}}{\text{PRF}}$	22.73 m/s

TABLE II
Specifications of equipment used

Parameter description	Value
C-band	5.5 GHz
Maximum transmit power	6.6 dBm
Bandwidth	28 MHz
Noise figure	3.8 dB
Antenna	10 dB

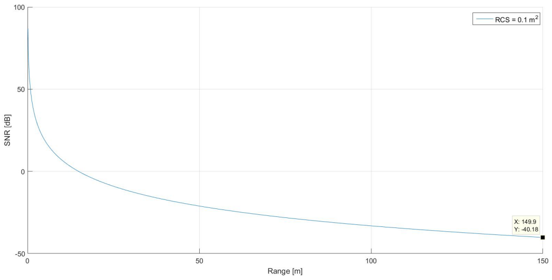

Fig. 3. SNR vs. range

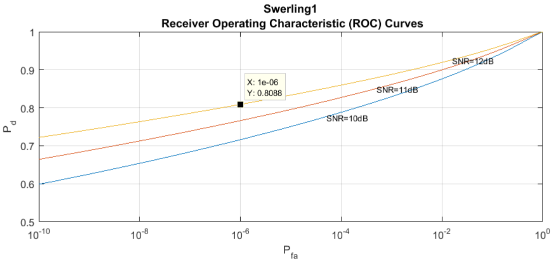

Fig. 4. ROC curve for various SNR values. The SNR of the detector performance requirement is 12 dB.

processing gain will be employed to improve the current SNR to equal the performance requirement.

1) Effect of Low-noise Amplifier (LNA): The HMC460 LNA is introduced to improve the noise figure of the system, thereby improving the SNR. The LNA has a noise figure of 2.5 dB and a gain of 14 dB. The effective noise figure is determined by cascading the noise factor of the receive chain using Frii's equation [9]:

$$NF(\text{dB}) = 10\log\left(F_1 + \frac{F_2 - 1}{G_1}\right), \tag{2}$$

where F_1 is the noise factor of the LNA, G_1 the gain of the LNA and F_2 is the noise factor of the USRP B210.

2) Effect of Power Amplifier: The TWAL 0412-20 amplifier was available, which is a 20 W amplifier with 43 dBm of power. The output power of the radar system is improved by 36 dB from the initial output power of 7 dBm.

3) Signal Processing Gain: The application of coherent integration can help to improve the SNR, since multiple pulses will be transmitted. The returned pulses n_p can be integrated coherently by adding the I and Q data, which is equivalent to increasing the SNR by a gain of $10 \log n_p$.

Fig. 5 shows the improvement obtained in SNR vs. range when implementing these measures.

IV. Implementation

Fig. 6 is the design for the radar system. The SDR approach allows less to be done in firmware but still builds on this technology by allowing the development to be done in software. The first step was to develop the independent GNU Radio block using C++ and Python that was responsible for generating the FMCW waveform using parameters of the waveform design. Fig. 7 shows the flow graphs of the implemented GNU Radio block. The B210 handles the transmit and receive waveform and GNU Radio applies the process of dechirping. The controller is embedded in the FMCW transmitter block. The data from the FMCW transmitter is written in real time and is passed as meta data via JSON (Java Script Object Notation) so that further signal processing steps that require the data can proceed. Further processing was done in Python, and the data packets were sent using the user datagram protocol (UDP). Detection and windowing were performed and the results displayed in a two-dimensional range and Doppler plot.

The UDP has a 65535 byte maximum size that can be transferred as a payload, 8 bytes is the UDP header and 20 bytes is the IP header. It affects the design since there is a bottleneck for data that can be processed at the same time. The range samples M was calculated to be 227 per pulse, when the pulse has PRF of 2200 Hz and the decimated sampling rate is 500 kHz. Since the data over UDP could not be complex, it was interleaved into float data which resulted in 454 samples being transferred over UDP. The waveform block was used to design the waveform, then the waveform was stored in a file using the GNU Radio file sink. The file source was used to

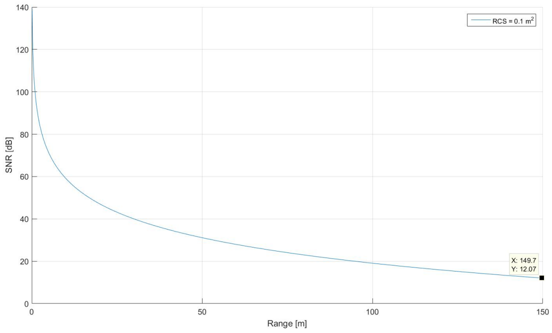

Fig. 5. SNR vs. range after implementing the LNA, power amplifier and pulse integration.

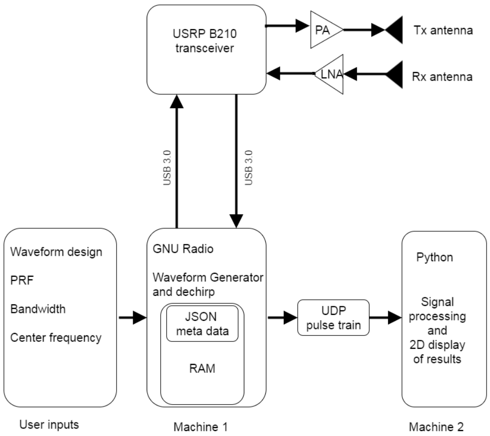

Fig. 6. Design for the radar showing how the user interacts with the system.

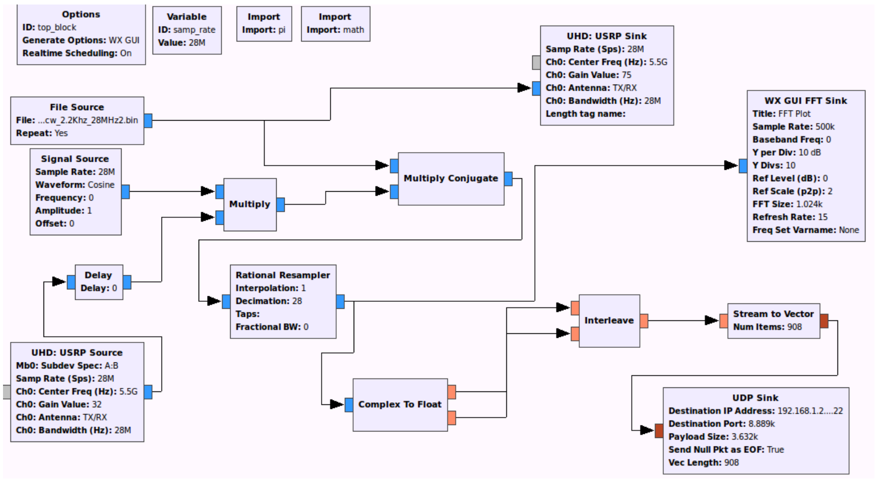

Options
ID: top_block
Generate Options: WX GUI
Realtime Scheduling: On

Variable
ID: samp_rate
Value: 28M

Import
Import: pi

Import
Import: math

File Source
File: ...cw_2.2Khz_28MHz2.bin
Repeat: Yes

Signal Source
Sample Rate: 28M
Waveform: Cosine
Frequency: 0
Amplitude: 1
Offset: 0

Delay
Delay: 0

UHD: USRP Source
Mb0: Subdev Spec: A:B
Samp Rate (Sps): 28M
Ch0: Center Freq (Hz): 5.5G
Ch0: Gain Value: 32
Ch0: Antenna: TX/RX
Ch0: Bandwidth (Hz): 28M

Multiply

Multiply Conjugate

Rational Resampler
Interpolation: 1
Decimation: 28
Taps:
Fractional BW: 0

Complex To Float

UHD: USRP Sink
Samp Rate (Sps): 28M
Ch0: Center Freq (Hz): 5.5G
Ch0: Gain Value: 75
Ch0: Antenna: TX/RX
Ch0: Bandwidth (Hz): 28M
Length tag name:

WX GUI FFT Sink
Title: FFT Plot
Sample Rate: 500k
Baseband Freq: 0
Y per Div: 10 dB
Y Divs: 10
Ref Level (dB): 0
Ref Scale (p2p): 2
FFT Size: 1.024k
Refresh Rate: 15
Freq Set Varname: None

Interleave

Stream to Vector
Num Items: 908

UDP Sink
Destination IP Address: 192.168.1.2....22
Destination Port: 8.889k
Payload Size: 3.632k
Send Null Pkt as EOF: True
Vec Length: 908

Fig. 7. GNU Radio implementation using the chirp signal which is displayed on the spectrum analyzer.

generate the waveform in real time and send the samples to the USRP.

The signal processing is done sequentially, as shown in Fig. 8. After receiving the meta data it is read from the JSON file that is shared over the network using Samba. The meta data sets the PRF, sampling rate, bandwidth, center frequency and the modulation waveform. The data is received from pulse to pulse and Hanning windowing is performed from pulse to pulse. According to the design, 50 pulses are received on which the two-dimensional FFT is performed. After the pulses have been coherently integrated, the result is displayed on an FFT plot. The pulses are arranged in a two-dimensional matrix and the windowing is done on the Doppler dimension together with the second FFT. The results are displayed on the two-dimensional Doppler range map.

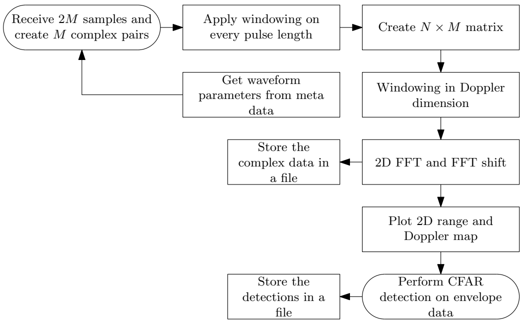
Receive $2M$ samples and create M complex pairs
Apply windowing on every pulse length
Create $N \times M$ matrix
Get waveform parameters from meta data
Windowing in Doppler dimension
Store the complex data in a file
2D FFT and FFT shift
Plot 2D range and Doppler map
Store the detections in a file
Perform CFAR detection on envelope data

Fig. 8. The signal processing algorithm.

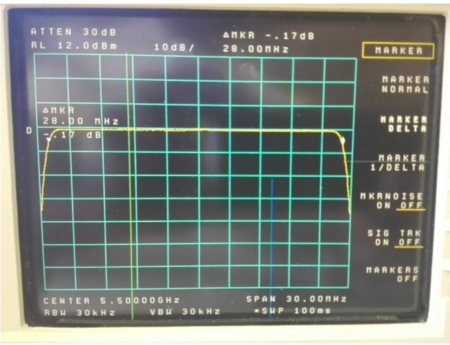

Fig. 9. Measured signal on the spectrum analyzer.

V. Results and Discussion

In order to validate the transmit waveform according to the design parameters, we used a computer with GNU Radio installed. This computer was responsible for generating the waveform, and was connected to the USRP transmitting the signal, which was measured on the spectrum analyzer. The measured signal on the spectrum analyzer showed that the bandwidth of the signal was 28 MHz, shown in Fig. 9 by ΔMkr, but the measured output power of the USRP was 1.39 dBm, and not the 6.6 dBm given in the specifications. The power of the signal is increased by the use of a power amplifier.

A human being and a car were used as targets in the experiments although the radar was designed to detect a drone. The experiments were done with reduced power: instead of the 43 dBm amplifier, a 13 dBm amplifier was used because of health implications and to account for using targets which have a bigger radar cross section (RCS) than a drone. Fig. 10 shows the setup and where the experiment was conducted.

The target is approximately 60 m from the radar. The target and the clutter are not moving, so it is expected that they should be at 0 m/s, but in Fig. 11 it is not centered at the 0 Hz Doppler bin due to the phase drift effect caused by the B210, the black line shows that the velocity is increasing with distance. The B210 contributes an unknown phase shift that varied with range on the range Doppler map.

To correct the phase drift, the phase correction algorithm shown in Fig. 12 was implemented in Python. The process was started by estimating the phase drift by calculating the slope of the phase drift. The Doppler shift is the rate of change of

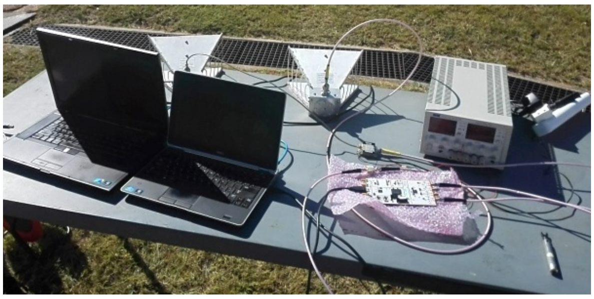

Fig. 10. Setup used for the experiments.

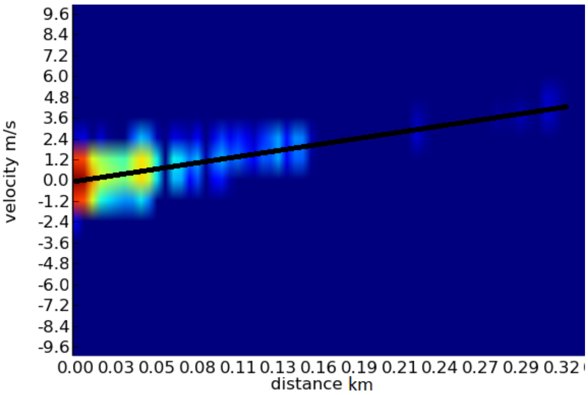

Fig. 11. Range Doppler map without phase correction with clutter and stationary target that was placed at approximately 60 m.

phase [9], which is calculated using:

$$\frac{\nabla \varphi}{2\pi} = \frac{2v}{\lambda PRF}. \tag{3}$$

The main aim of creating the equalization matrix was to create a negative slope with the same phase drift as the range Doppler matrix that had to be corrected. The phase drift was assumed to increase linearly, thus the equalization matrix was implemented in such a way that its phase drift increases linearly. The process of creating the 2D equalization matrix starts by creating a 1D array, with the data in increments of phase correction angle φ. The 1D array is transformed to 2D by incrementing the phase by the pulse number on the Doppler dimension—in the design 50 pulses were used for Doppler processing, thus the equalization matrix should be populated with 50 pulses so that the sizes are the same.

The data from the experiment was saved in a 2D FFT matrix, thus when it is read it undergoes inverse fast Fourier transform (IFFT) to get back to the time domain. Element-wise multiplication is performed between the experimental data and the equalization matrix, which has complex cosine and sine pairs. This will only cause phase change on the experimental data without affecting the amplitude, as can be shown using the Fourier transform pair [9]:

$$e^{j2\pi f_0 t} x[n] \longleftrightarrow X[f - f_0]. \tag{4}$$

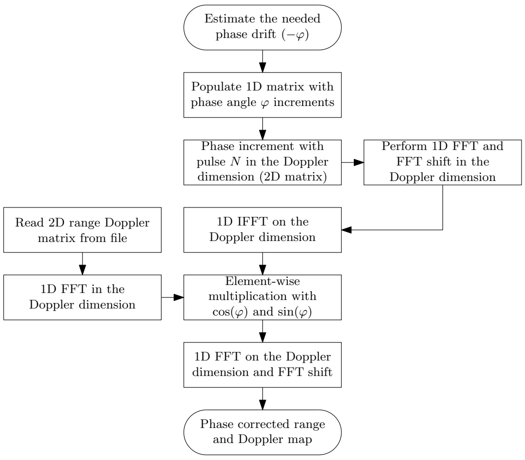
Estimate the needed phase drift ($-\varphi$)
Populate 1D matrix with phase angle φ increments
Phase increment with pulse N in the Doppler dimension (2D matrix)
Perform 1D FFT and FFT shift in the Doppler dimension
Read 2D range Doppler matrix from file
1D IFFT on the Doppler dimension
1D FFT in the Doppler dimension
Element-wise multiplication with cos(φ) and sin(φ)
1D FFT on the Doppler dimension and FFT shift
Phase corrected range and Doppler map

Fig. 12. Phase correction algorithm flow graph.

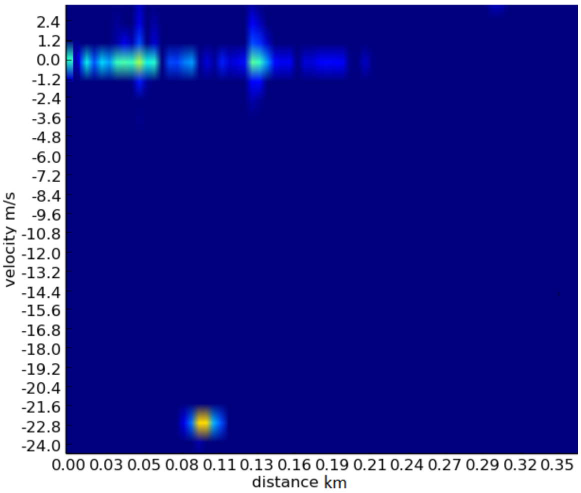

Fig. 13. Range Doppler map showing a car moving away from the radar. This is to test the radar for high speed.

After performing the element-wise multiplication in the time domain, the results are transformed back into the frequency domain and viewed on the range Doppler map.

In Fig. 13 we can see the car at the velocity of approximately 20 m/s when the car was moving away from the radar. The phase drift has been corrected—there is no longer a slope or clutter, and the target has 0 Hz Doppler shift.

A. Probability of Detection Performance and Verification

In order to confirm the probability of detection a human was placed at a range of approximately 150 m, as it was specified from the user requirement for probability of detection of 80%. A number of trials should be repeated and saved to file to determine how many times the radar is able to detect the target; 1000 trials were performed. The human target was going back and forth in a circular motion within a distance of 5 m so that on the detector it will appear on the 28-th range bin. This will cause the RCS of the target to fluctuate since the range resolution of the radar is 5.35 m and the target is moving in the range bin.

The target was detected 639 times out of the 1000 trials. The achieved P_d is 63.9%, but the expected probability of detection is 80%:

$$P_d = \frac{N_{\text{detections}}}{N_{\text{trials}}}. \tag{5}$$

We use the Gaussian approximation to determine the confidence interval [11], where P is the mean of P_d, N is the number of trials and z is the critical value given for various values of probability:

$$x_L, x_u = P \pm z\sqrt{\frac{P(1-P)}{N}},$$
$$x_L, x_u = 0.639 \pm 0.013.$$

The reason why the detector could not perform optimally is that the strong signal return from the close-by objects may have masked the weak signal return from the target of interest as the RCS changes. From the design we could not meet the range resolution specification of 0.1 m for the RCS of 0.1 m^2 target, the range resolution that was achieved is 5.35 m. This results in more clutter energy being integrated into a single cell along with the target, thus affecting the achieved SNR.

B. *Probability of False Alarm Performance Verification*

The other performance specification that needs to be met is the probability of false alarm. To do that the radar is directed in the vertical direction so that the radar only measures the leakage, thermal noise and opportunistic signals within the vicinity of the radar. A 100 trials of measurements are to be recorded, then we will use the constant false alarm rate (CFAR) detector to estimate the rate of false detections. The CFAR detector dynamically adjusts the threshold and, thus, it is not expected that noise will cause any false alarms. However, the system can generate spurious signal or receive opportunistic signals, thus once in a while a false target will be detected.

As a rule of thumb the value N should be at least $N \geq 10/P_{fa}$, resulting in 100000000 trials [11]. Lower values of N can still be used and relate it to time [9]:

$$P_{fa} = \frac{T_m FAR}{M}, \tag{6}$$

where FAR is the false alarm rate (i.e. how many false alarms occur in a second) and T_m is the time interval at which the number of resolution cells M are collected. Each trial consists of 226 samples of data, which represents a pulse at a PRF of 2200 Hz. The data capture was repeated for 100 trials. The calculated P_{fa} is 1.7×10^{-6}, which is a good enough approximation for 1 false detection for 1 million radar observations.

VI. Conclusion

Drones are becoming popular for varying applications, but they are also being used for illegal activities such as spying and flying into restricted areas, thus a study of surveillance radar using SDR (i.e. GNU Radio and B210) was done since it can be a portable and cost efficient solution.

A radar was designed and modeled using the given user requirements and performance specifications. The radar was expected to detect a drone up to 150 m away with 80% probability of detection and 10^{-6} probability of false alarm. The USRP B210 is part of the user requirements, and it had to be used as transceiver. It was studied in order to understand how it performs and what its limitations are. The waveform designed has PRF of 2200 Hz, at a center frequency of 5.5 GHz and bandwidth of 28 MHz; this results in resolution of 5.35 m, maximum unambiguous velocity of 30 m/s and velocity resolution of 1.2 m/s when 50 pulses are used for Doppler processing. The system was only capable of reaching 63.9% probability of detection and 1.7×10^{-6} probability of false alarm.

The bandwidth was still a limiting factor in terms of range resolution; however, reading the waveform from the file made it possible to increase the resolution. According to the specifications of the B210, 56 MHz of instantaneous bandwidth can be achieved, but in the implementation only 28 MHz was achieved when both transmitter and receiver channels were used. The phase drift caused by the local oscillator of the B210 is one of the limiting factors in terms of getting an accurate Doppler shift. During the experiments a Doppler shift was induced, so a phase correction algorithm was implemented to solve the issue by creating an equalization matrix.

References

[1] J. Marimuthu, K. S. Bialkowski and A. M. Abbosh, “Reconfigurable Software Defined Radar for medical imaging,” in *Australian Microwave Symp.*, Melbourne, Australia, Jun. 26–27, 2014, pp. 15–16.

[2] D. M. Chinnam, J. Madhusudhan, C. Nandhini, S. N. Prathyusha, S. Sowmiya, R. Ramanathan and K. P. Soman, “Implementation of a low cost synthetic aperture radar using software defined radio,” in *Int. Conf. Computing Commun. Netw. Technol.*, Karur, India, Jul. 29–31, 2010, pp. 1–7.

[3] J. Ralston and C. Hargrave, “Software defined radar: An open source platform for prototype GPR development,” in *Int. Conf. Ground Penetrating Radar*, Shanghai, China, Jun. 4–8, 2012, pp. 172–177.

[4] S. Sundaresan, C. Anjana, T. Zacharia and R. Gandhiraj, “Real time implementation of FMCW radar for target detection using GNU radio and USRP,” in *Proc. Int. Conf. Commun. Signal Proc.*, Melmaruvathur, India, Apr. 2–4, 2015, pp. 1530–1534.

[5] A. Prabaswara, A. Munir and A. B. Suksmono, “GNU Radio based software-defined FMCW radar for weather surveillance application,” in *Int. Conf. Telecommun. Syst. Services Applic.*, Bali, Indonesia, Oct. 20–21, 2011, pp. 227–230.

[6] M. Inggs, G. Inggs, A. Langman and S. Scott, “Growing horns: Applying the Rhino software defined radio system to radar,” in *IEEE Radar Conf.*, Kansas City, MO, May 23–27, 2011, pp. 951–955.

[7] (2016, June 26). Accurately detect and locate drones and their operators. Available: https://www.echoradarsystems.com/drone-detection-system/

[8] H. Rohling and M. Kronauge, “New radar waveform based on a chirp sequence,” *Int. Radar Conf.*, Lille, France, Oct. 13–17, 2014, pp. 1–4.

[9] M. A. Richards, J. A. Scheer and W. A. Holm, *Principles of Modern Radar: Basic Principles*, SciTech Publishing, 2010.

[10] D. E. Barrick, “FM/CW radar signals and digital processing,” *NOAA Technical Report ERL 283-WPL 26*, 1973.

[11] J. D. Echard, “Estimation of radar detection and false alarm probability,” *IEEE Trans. Aerosp. Electron. Syst.*, vol. 27, no. 2, pp. 255–260, Mar. 1991.